

# Near-perfect hologram reconstruction with a spatial light modulator

Alexander Jesacher, Christian Maurer, Andreas Schwaighofer,  
Stefan Bernet and Monika Ritsch-Marte

Division for Biomedical Physics, Innsbruck Medical University, Müllerstrasse 44  
A-6020 Innsbruck, Austria

[Alexander.Jesacher@i-med.ac.at](mailto:Alexander.Jesacher@i-med.ac.at)

**Abstract:** We present an implementation method for noiseless holographic projection of precalculated light fields with a spatial light modulator. In the reconstructed image, both the spatial amplitude and phase distributions can be programmed independently. This is achieved by diffracting the light from two successive phase holograms that are located in conjugate Fourier planes. The light path is folded such that the two corresponding phase masks can be displayed side by side at a single phase-only spatial light modulator. Such a device has relevant applications in holographic display- or projection systems, and for optical micromanipulation in laser tweezers.

© 2008 Optical Society of America

**OCIS codes:** (090.1995) Digital holography; (230.6120) Spatial light modulators

---

## References and links

1. P. Hariharan, *Optical Holography: Principles, Techniques, and Applications* (Cambridge University Press, 1996).
2. B. Kress and P. Meyrueis, *Digital diffractive optics* (Wiley, 2000).
3. H. Kim, K. Choi, and B. Lee, "Diffractive Optic Synthesis and Analysis of Light Fields and Recent Applications," *Jpn. J. Appl. Phys.* **45**, 6555–6575 (2006).
4. M.-L. Hsieh, M.-L. Chen, and C.-J. Cheng, "Improvement of the complex modulated characteristic of cascaded liquid crystal spatial light modulators by using a novel amplitude compensated technique," *Opt. Eng.* **46**, 07501 (2007).
5. J. P. Kirk and A. L. Jones, "Phase-Only Complex-Valued Spatial Filter," *J. Opt. Soc. Am.* **61**, 1023–1028 (1971).
6. C. Maurer, A. Jesacher, S. Fürhapter, S. Bernet, and M. Ritsch-Marte, "Tailoring of arbitrary optical vector beams," *N. J. Phys.* **9**, 78 (2007).
7. H. Bartelt, "Computer-generated holographic component with optimum light efficiency," *Appl. Opt.* **23**, 1499–1502 (1984).
8. H. O. Bartelt, "Applications of the tandem component: an element with optimum light efficiency," *Appl. Opt.* **24**, 3811–3816 (1985).
9. Y. Roichman and D. G. Grier, "Projecting extended optical traps with shape-phase holography," *Opt. Lett.* **31**, 1675–1677 (2006).
10. G. O. Reynolds, J. B. Develis, and B. J. Thompson, *The New Physical Optics Notebook: Tutorials in Fourier Optics* (SPIE, 1989).
11. R. W. Gerchberg and W. O. Saxton, "A practical algorithm for the determination of phase from image and diffraction plane pictures," *Optik* **35**, 237–246 (1972).
12. S. Chu, J. E. Bjorkholm, A. Ashkin, and A. Cable, "Experimental observation of optically trapped atoms," *Phys. Rev. Lett.* **57**, 314–317 (1986).
13. D. McGloin, G. Spalding, H. Melville, W. Sibbett, and K. Dholakia, "Applications of spatial light modulators in atom optics," *Opt. Express* **11**, 158–166 (2003).
14. J. Liesener, M. Reicherter, T. Haist, and H. J. Tiziani, "Multi-functional optical tweezers using computer-generated holograms," *Opt. Commun.* **185**, 77–82 (2000).
15. A. Jesacher, C. Maurer, S. Fürhapter, A. Schwaighofer, S. Bernet, and M. Ritsch-Marte, "Optical tweezers of programmable shape with transverse scattering forces," *Opt. Commun.* (to be published).

## 1. Introduction

In principle computer generated holography (CGH) should be easy: in order to obtain a perfect reconstruction of any precalculated light field distribution one just has to “somehow imprint” the two-dimensional Fourier transform of the desired holographic image (optionally superposed with a parabolic phase term to control the imaging distance) onto an incoming wave.

However, in practice the “imprinting process” is difficult. One reason for this is that the two-dimensional Fourier transform of an image is generally *complex*, which means that both the amplitude and the phase of an incoming wave have to be controlled, while display elements for holographic reconstruction, like CGHs or real-time programmable spatial light modulators (SLMs) are typically phase-only modulators.

Although there are ways to encode light fields in a single phase-only diffractive optical element (DOE) [1, 2, 3], it generally turns out that this requires serious trade-offs, producing for example increased speckle noise and loss of independent control over amplitude and phase of the reconstructed light field.

On the other hand exist methods where both, the amplitude and the phase of the incoming light wave are modulated, for example by using sophisticated photographic materials to produce *referenceless on-axis complex holograms (ROACH)* [1], or more recently, by using a phase and an amplitude SLM cascaded in a 4-f-system [4]. Further possibilities are to control the intensity of the diffracted light by modifying the local grating depth of an off-axis phase DOE [5, 6], or by properly dividing a DOE into assigned and unassigned regions [9]. However, typical Fourier holograms usually exhibit a huge intensity contrast of several orders of magnitude between their central zero-order Fourier component, and the outer higher-order components. Techniques which shape such a high contrast amplitude profile with an absorptive mask from a uniform beam sacrifice most of the intensity.

Here we present a SLM-based practical realization of an approach, which was introduced in 1984 by H. Bartelt [7, 8]. The method allows to shape arbitrary complex light fields by using two subsequently arranged phase DOEs. Instead of producing the amplitude modulation with an absorbing mask, this is achieved by redistributing the intensity of an incoming beam by on-axis diffraction at a first phase-hologram. This projects the desired precalculated amplitude modulation with a theoretically unlimited high contrast, and without sacrificing any light intensity, to a second phase-only display, which adjusts the phases of the respective Fourier components. Thus behind the second phase mask the full *complex* amplitude of a precalculated field distribution is generated. Such a complete complex modulation produces a speckle-free hologram readout where both, the amplitude and the phase of the reconstructed image can be adjusted independently. Although the hologram is reconstructed “on-axis”, the generated light field contains no undesired contributions from other diffraction orders, and no disturbing zero-order Fourier spot often appearing in non-optimized DOEs. Since, in principle, no light is absorbed, the whole incoming intensity is used for imaging, and the theoretically obtainable efficiency is 100%.

So far, implementations of this technique used static diffractive elements, such as bleached films [8], the production of which is relatively complex and time consuming. Here we experimentally demonstrate the feasibility of creating arbitrary complex light fields of high quality with real-time programmable SLMs. Our proposed setup requires only one single SLM, which displays both required diffractive patterns side by side. Moreover, we show that image reconstruction is even possible, if the two phase masks are only binary. This allows one to use the method also with ferroelectric SLMs, which offer only binary phase modulation, but have the advantage of a very high switching speed.

## 2. Principle of the method

Figure 1 outlines the principle of the technique schematically. The method requires two phase diffractive elements, placed in conjugate Fourier planes in the beam path (planes referred to as “plane 1” and “Fourier plane” in the figure), which means that the light fields in these planes are mathematically “connected” by the Fourier transform [10]. In the figure, the two elements are referred to as  $P1$  and  $P2$ , respectively. The complex fields in the planes directly before and after  $P2$  are each represented by two images, showing the actual amplitude and phase.

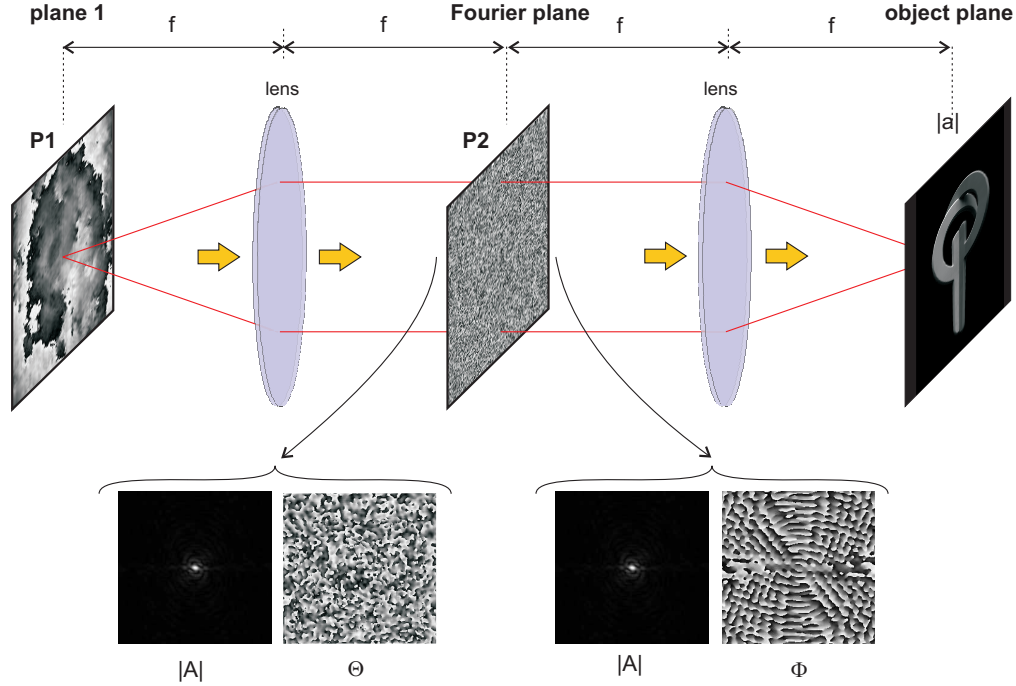


Fig. 1. Principle of the method. A specific complex light field in the object plane (right plane) is created by two phase-diffractive patterns ( $P1$  and  $P2$  – gray shades in the figure correspond to phase values from 0 to  $2\pi$ ), which are placed in two conjugate planes (plane 1 and the Fourier plane).  $P1$  is iteratively optimized to create the amplitude  $|A|$  in the Fourier plane. There, the desired phase function  $\Phi$  is shaped from the “noisy” phase  $\Theta$  by pattern  $P2$ .

Let us assume that one wants to create a specific light field  $a(x,y)$  in the object plane (plane on the right). In our example, the amplitude of this specific light field has the shape of our department logo, and we chose its phase to be uniform. The creation of the field  $a(x,y) = |a(x,y)| \exp[i\phi(x,y)]$  in the object plane demands a definite complex field  $A(u,v) = |A(u,v)| \exp[i\Phi(u,v)]$  in the Fourier plane (right pair of images in the Fourier plane), which can be expressed as:

$$A(u,v) = \frac{1}{\lambda f} \int_x \int_y a(x,y) \exp \left[ -i \frac{2\pi}{\lambda f} (ux + yv) \right] dx dy. \quad (1)$$

Here,  $\lambda$  is the laser wavelength and  $f$  the focal length of the Fourier-transforming lens.

The phase of the field  $A(u,v)$  could be directly shaped by the element  $P2$  in the Fourier plane, but not its amplitude. Thus the amplitude of  $A(u,v)$  must be created by  $P1$ , which is located

in plane 1.  $P1$  can be iteratively optimized using specific phase DOE design algorithms [2], such that it creates the desired modulus  $|A(u, v)|$  in the Fourier plane when it is homogeneously illuminated. This even works if  $|A(u, v)|$  exhibits very high contrast, as typical for Fourier holograms. However, a consequence of this optimization procedure is that the field created by  $P1$  in the plane  $P2$  will have a randomly distributed phase  $\Theta(u, v)$ . Generally this “noisy” phase will not correspond to the demanded phase function  $\Phi(u, v)$ . Although the phase  $\Theta(u, v)$  cannot be controlled, since it is used as the optimization parameter to create  $|A(u, v)|$ , it is known. Now the idea is to modify  $\Theta$  by  $P2$  such that the result is  $\Phi(u, v)$ . Consequently,  $P2$  has to be calculated as follows:

$$P2 = \text{mod}2\pi\{\Phi - \Theta\}, \quad (2)$$

where  $\text{mod}2\pi\{\dots\}$  symbolizes the “modulo-” operation that restricts the phase of  $P2$  to an interval between 0 and  $2\pi$ . Altogether, this procedure generates the desired complex field  $A(u, v)$  directly behind the second phase mask  $P2$ , and hence also  $a(x, y)$  in the object plane. Theoretically, no light is lost since the method solely utilizes non-absorbing phase elements.

### 3. Experimental setup and results

Figure 2 illustrates how this concept can be realized with a single SLM. For our experimental work, we utilized a *HEO 1080* parallel aligned nematic SLM from *Holoeye Photonics AG*, which is a pure phase modulator with an active area of approximately  $2 \times 1 \text{ cm}^2$ , consisting of  $1920 \times 1080$  pixels. Each pixel measures  $8 \times 8 \mu\text{m}^2$ . The display has a light utilization efficiency (defined as the power ratio of zeroth diffraction order to incident beam when no pattern is displayed) of 55%, which is mainly determined by absorption. Typical values of the zeroth and first diffraction orders of displayed phase structures are 6% and 41%, respectively. The values represent power ratios of the according diffraction order to incident light and correspond to a 10 pixel sawtooth grating (measured values). The zeroth order is mainly caused by the limited fill factor of the SLM.

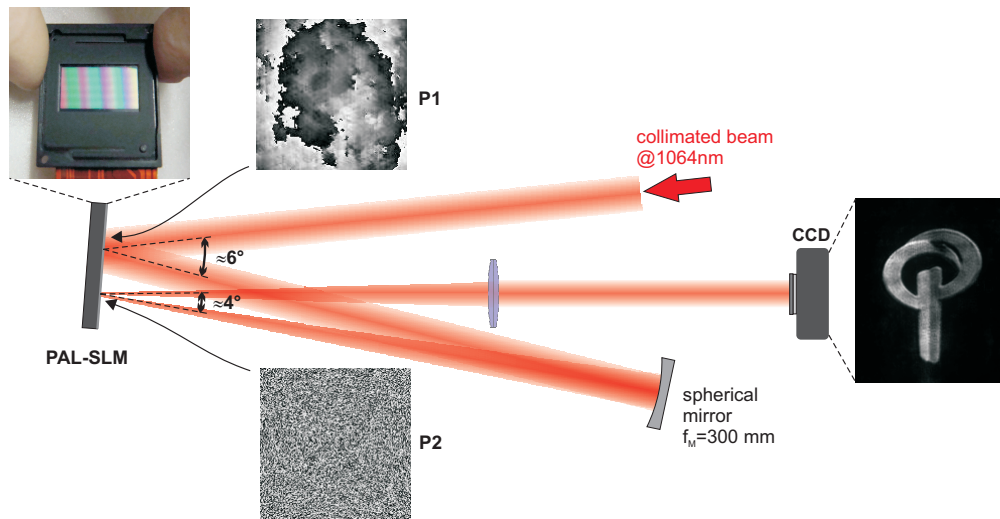


Fig. 2. Sketch of the experimental setup. The phase patterns  $P1$  and  $P2$  are displayed side by side at the phase modulator panel. The light diffracted from  $P1$  is reflected back onto  $P2$  by a slightly tilted concave mirror, which additionally performs the optical Fourier transform.  $P2$  rearranges the light phase and creates the desired phase function.

The two patterns  $P1$  and  $P2$  (each measures  $960 \times 960$  pixels) are displayed side by side at the modulator panel. Almost all pixels can be used to display the square patterns, since the panel dimensions show a relation of 16:9.  $P1$  was obtained by 15 iterations of the Gerchberg-Saxton algorithm [11]. It is illuminated by an expanded and collimated Ytterbium fiber laser (horizontally polarized) emitting at  $\lambda=1064$  nm. No polarizers are used in the present configuration. The diffracted laser is subsequently reflected onto  $P2$  by a concave mirror, such that the desired modulus  $|A(u, v)|$  emerges in the plane of  $P2$ . There  $P2$  shapes the demanded phase function  $\Phi(u, v)$  from the noisy, but known, wavefront of the incoming wave. Finally, the resulting complex field is again Fourier transformed by an imaging lens such that the desired light field appears at the CCD (DVC-1412 camera). In the present configuration, the two subsequent diffraction processes restrict the maximal obtainable diffraction efficiency to only about 17%, which is mainly determined by the absorption of our SLM, but not by fundamental reasons. The red beam in the sketch of Fig. 2 indicates the laser path if the SLM is switched off, i.e. when it acts as a mirror. This path is identical to that of the zeroth diffraction orders of  $P1$  and  $P2$ .

Strictly speaking, Eq. 1 is not applicable for the experimental situation described in Fig. 2, since the pattern planes and the concave mirror are slightly tilted with respect to their counterparts in Fig. 1. However, the tilt angles are very small (maximal 3 degrees), and hence allow abandoning a corresponding modification of Eq. 1 without considerable quality reduction. A crucial point for achieving good holographic reconstructions is the accurate alignment of  $P2$ , which should be exact within a few microns. In the experiment the alignment can be achieved without mechanical tools by electronically shifting the phase masks across the SLM display. The sensitivity of image quality to misalignments is determined by  $f_M$ , the focal length of the concave mirror, since this parameter determines the highest possible spatial frequency of the “noisy” phase  $\Theta(u, v)$ . A relative short focal length  $f_M$  leads to high spatial noise frequencies

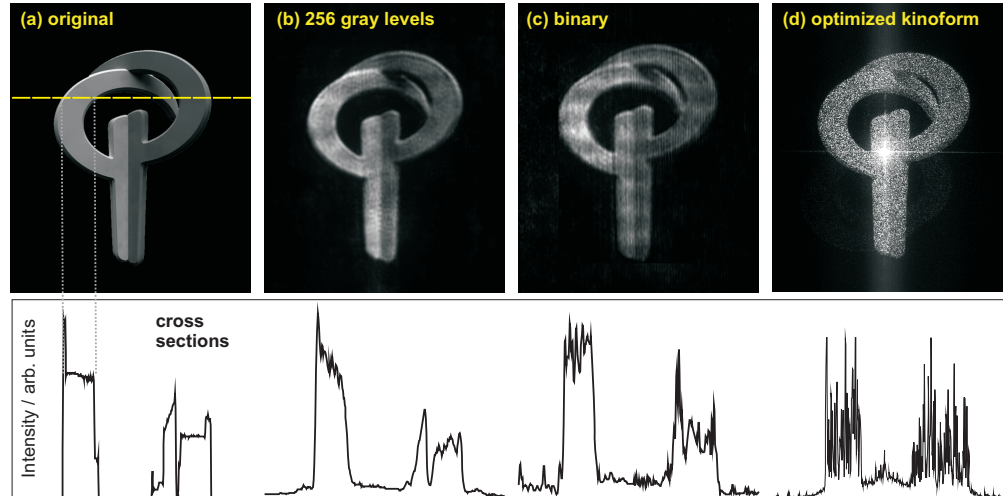


Fig. 3. Holographical reconstructions of a gray-scale image. (a) represents the original. (b) and (c) have been created with the presented method, using 256 or 2 distinct phase levels for displaying the phase patterns, respectively. (d) shows the experimental reconstruction of the image from a single optimized phase DOE (256 phase levels) for comparison. Clearly visible are the “noisy” texture and the zero diffraction order, which is represented by the intense spot in the image center. The plots below the images show the individual intensities along a definite cross section (indicated by the yellow dashed line in (a))



and hence to a high sensitivity to misalignment, but, on the other hand, increases the resolution of the reconstructed amplitude  $|A(u, v)|$ . Furthermore, the angles of incidence of the beam to the display should be as small as possible. According to our experience, good results can be achieved with  $f_M=300$  mm.

A translation of the phase mask  $P1$  across the SLM screen does not result in an image degradation, but just in a corresponding translation of the reconstructed image in the camera plane. This is due to the Fourier-shift theorem, which assures that a transverse shift of  $P1$  does not lead to a shift of the reconstructed amplitude pattern  $|A(u, v)|$  in the plane  $P2$ , but just to a linear phase-offset of this pattern, which, due to the subsequent Fourier transform, finally translates into a lateral image shift in the observation plane.

Figure 3 demonstrates the performance of the experimental setup. It shows three holographic reconstructions of our department logo, which have been created using different methods. The gray-scale image on the left (a) represents the original logo. (b) is a holographically reconstructed image that was created by exploiting all available phase levels of our 8-bit display.  $P1$  and  $P2$  were calculated “on-axis”, which in the case of “normal” Fourier-holograms typically leads to contributions of undesired diffraction orders, i.e. a bright spot of the zero order in the center. However, image (b) shows that this undesired effect does not occur in our setup. The measured light efficiency was 15%. The patterns used for this experiment are printed in Fig. 2 as small gray scale images.

The third image (c) was created by “binarizing” the patterns used in (b) and hence demonstrates the applicability of the method to binary ferroelectric SLMs. Here, both patterns were calculated “off-axis” in order to avoid image degradation by the now intense conjugate and zero diffraction orders. The measured light efficiency was 1.5%. Finally, the logo on the right (d) was shaped by a single kinoform, which has been optimized using the Gerchberg-Saxton algorithm [11]. The efficiency was close to the theoretical maximum. However, the image clearly shows the typical “noisy” texture of a kinoform image, which is caused by the randomized phase, and an intense zero order spot near the center.

A first step for using this setup for three-dimensional holographic display- or projection tasks is to reconstruct two objects in two distinct axial planes. This is demonstrated in Fig. 4. The left image is a holographic reconstruction of an image containing a rabbit and an eagle, both in focus and (virtually) having an infinite distance to the camera. Then the hologram was recalculated, adapting the two phase masks at the SLM, such that the eagle had a virtual distance

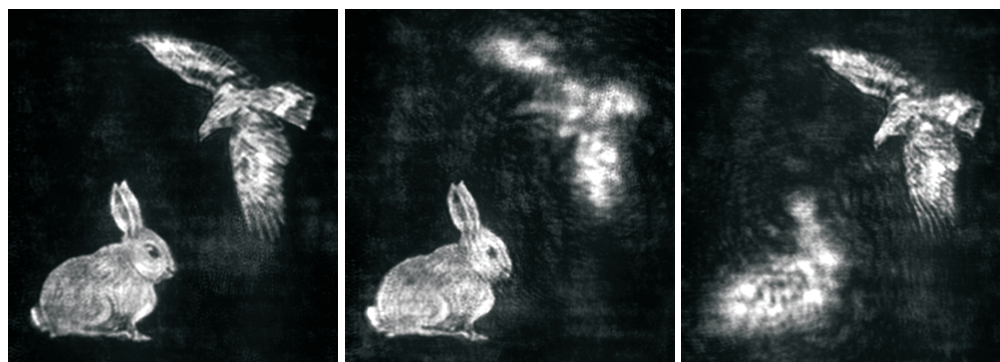


Fig. 4. Left: Images of a rabbit and an eagle are reconstructed in a common axial plane. Thus both animals appear sharply. Middle and right image: The rabbit and the eagle emerge in two distinct axial planes. Different focus settings allow to see only one animal sharply at a time, while the other one appears blurred.

of now only about one meter from the camera. As a consequence, the eagle appears blurred in the middle image of Fig. 4. Finally, the camera was focussed on the eagle (right image) which leads simultaneously to a defocussing of the rabbit.

#### 4. Summary and discussion

We have presented an SLM-based implementation of a method to create complex holograms using two cascaded phase DOEs. Compared to existing techniques, the method shapes the amplitude profile by pure phase elements, which allows a theoretical light efficiency of almost 100%. In addition, high contrast amplitudes, which usually appear in Fourier holograms [1], can be easily created. Although there are alternative methods to create speckle-free complex light fields with a single phase diffractive pattern (for instance via a confined reconstruction area), they are not lossless and imply side-effects such as the appearance of sometimes undesired light in higher diffraction orders.

Our implementation requires only a single SLM, which displays both diffractive patterns side by side. We have compared the resulting image quality with that of an optimized kinoform. Furthermore, we have demonstrated the feasibility of the technique in view of binary DOEs, such as ferroelectric SLMs. In the present SLM configuration, the theoretically obtainable light efficiency was limited by the absorption of the SLM display to about 17%. However, a value close to this theoretical maximum was also experimentally achieved, which indicates that the efficiency of an implementation with ideal DOEs would be close to 100%.

The possibility to project light with full efficiency into precalculated amplitude and phase fields has many practical applications. First, the method leads to speckle-free images, since speckles arise as a consequence of a speckled object phase and the discarded amplitude in standard phase holograms, kinoforms, or DOEs. Second, in holographic display- or projection systems, shaping not only the intensity but also the phase distribution of the reconstructed image allows one to control the light field also in out-of-focus planes. For example, an image area with a flat phase profile has a large depth of sharpness – such areas will be sharply visible even in out-of-focus observation planes. On the contrary, image areas with a noisy phase distribution have a low depth of focus and will be sharply reconstructed only in focus. Phase shaping also allows to determine the divergence and the direction of light behind (or in front) of the sharp image plane. Altogether this is the basis to create holograms of artificial objects with different surface textures, like specular or diffuse reflecting areas.

Furthermore, independent intensity and phase control of reconstructed light fields is the basis for artificial holography of *three-dimensional* objects. Since it is possible to generate any desired light field distribution in the plane behind the second DOE, it is clear that also the light field emitted from a real three-dimensional object can be simulated, and an observer will just see the corresponding virtual object. The high efficiency of the projected light fields also suggests applications for optical trapping and micromanipulation in atom traps [12, 13] or diffractive laser tweezers [14]. Controlling phase and amplitude of the trapping light field means to have full control over the exerted scattering and gradient forces. For example, the scattering force of light pushes particles in the direction of its phase gradient. Therefore the possibility to project line patterns with a tailored transverse phase gradient allows to move particles along precalculated pathways, even within static light fields [15].

#### Acknowledgments

This work was supported by the Austrian Science Foundation (FWF), Project No. P18051-N02 and Project No. P19582.